# Lateral Interactions in the Dissociation Kinetics of NO on Rh(100)†

**M. J. P. Hopstaken and J. W. Niemantsverdriet***

*Schuit Institute of Catalysis, Eindhoven University of Technology, P.O. Box 513, 5600 MB Eindhoven, The Netherlands*

*Received: September 9, 1999; In Final Form: November 11, 1999*

Temperature programmed desorption and static secondary ion mass spectrometry have been used to study the dissociation and desorption of NO and the formation of $N_2$ on the (100) surface of rhodium. At low coverages we find an activation energy of 37 ± 5 kJ/mol for dissociation of NO and 225 ± 5 kJ/mol for $N_2$ desorption. At higher coverages the dissociation is significantly retarded by lateral interactions with N- and O-atoms and NO molecules. At coverages close to saturation the dissociation is entirely blocked by NO due to the lack of ensembles containing empty sites. The results are compared with those of earlier studies on Rh(111). It appears that dissociation of NO proceeds faster on the more open Rh(100) surface, due to the higher heat of adsorption of the N-atoms. As a consequence, formation of $N_2$ is slower than on Rh(111).

## I. Introduction

Rhodium is a major constituent of the automotive exhaust gas converter, owing to its properties to convert NO to $N_2$ with high selectivity.[1,2] Adsorption and dissociation of NO has been the subject of studies on polycrystalline Rh[3−6] and on the three low Miller index surfaces: Rh(111),[7−18] Rh(100),[19−25] and Rh(110).[26−31] The results generally indicate that NO adsorbs molecularly at low temperature but dissociates upon heating. At low coverage, NO dissociates completely as evidenced by $N_2$ formation between 450 and 800 K, depending on the surface orientation, whereas $O_2$ desorbs at much higher temperatures (1000−1400 K). At higher initial coverages of NO, however, dissociation is incomplete, as indicated by desorption of up to half of the originally present NO between 400 and 450 K. Using a combination of temperature programmed desorption (TPD) and static secondary ion mass spectrometry (SIMS), Borg et al.[13] showed that the dissociation of NO on Rh(111) shifts to higher temperatures with increasing coverage. At saturation coverage, dissociation is blocked completely until the temperature is reached where NO desorbs. The coverage dependence of the NO dissociation rate points to the requirement of an ensemble of unoccupied rhodium atoms for dissociation, as predicted on the basis of theoretical calculations,[32−34] although repulsive lateral interactions are expected to increase the activation energy for dissociation as well.[35]

The kinetics of dissociation reactions, as well as that of any surface reaction involving adsorbed atoms, notably $N_2$ formation, depends for a given metal strongly on the structure of the surface. Therefore, a detailed study of the NO dissociation on Rh(100) and a comparison with the results on Rh(111) are clearly of interest with respect to the kinetic modeling of NO reduction reactions such as the NO + CO and NO + $H_2$ reactions on automotive exhaust catalysts.

Only a few studies dealing with the dissociation of NO on Rh(100) exist. Villarubia et al.,[22] using temperature programmed electron energy loss spectroscopy, report kinetic parameters ($E_{dis}$ = 44 kJ/mol and $\nu_{dis} = 10^{11}$ $s^{-1}$) for dissociation of NO on Rh(100). These values, however, were derived on the assumption that dissociation is first order in NO coverage only, with no further effect of surface coverage through ensemble requirements or lateral interactions. A preliminary SIMS study by Siokou et al.[24] indicates that NO decomposition on Rh(100) depends as much on coverage as it does on Rh(111), be it that the dissociation proceeds at lower temperatures. Nitrogen formation was observed at significantly higher temperatures than on the (111) surface, however. A theoretical study by Shustorovich and Bell[36] has reproduced the strong coverage dependence of the NO dissociation rate.

A point of debate is the existence of more than one formation channel for $N_2$ on Rh(100). TPD measurements of NO on Rh(100) reveal two $N_2$ desorption regimes, one corresponding to second-order recombination of N-atoms at 600−800 K and another coincident with desorption of NO between 400 and 430 K. The latter has been taken as evidence for a disproportionation reaction between NO and N to yield $N_2$ and an adsorbed O-atom.[18,22,24] A similar mechanism proposed to explain a low-temperature $N_2$ desorption state on Rh(111) could be discounted in an isotopic study by Belton et al.[37] We present conclusive evidence in this paper that the low-temperature $N_2$ desorption peak on Rh(100) is an artifact caused by decomposition of NO at hot filaments.

In this paper we present a detailed study on the dissociation of NO on Rh(100) by monitoring surface coverages during reaction with static SIMS and TPD. A simple model will be introduced to describe the coverage dependence of the kinetic parameters. Finally we compare the results with the kinetics of NO dissociation on Rh(111) as presented in earlier studies from our laboratory.[13,35]

## II. Experimental Section

The experiments were done in a stainless steel ultrahigh vacuum (UHV) system with a base pressure of $10^{-10}$ mbar, as previously described by Borg et al.[13] Static SIMS spectra were taken by using a defocused 5-keV $Ar^+$ primary ion beam with a current density of 1 nA/$cm^2$ at an incident polar angle of 60° with respect to the surface normal. Secondary ions were

† Part of the special issue "Gabor Somorjai Festschrift".

* Corresponding author. Telephone: +0031 40 247 3067. Fax: +0031 40 245 5054. E-mail: J.W.Niemantsverdriet@tue.nl.

10.1021/jp993200+ CCC: $19.00 
Published on Web 01/04/2000

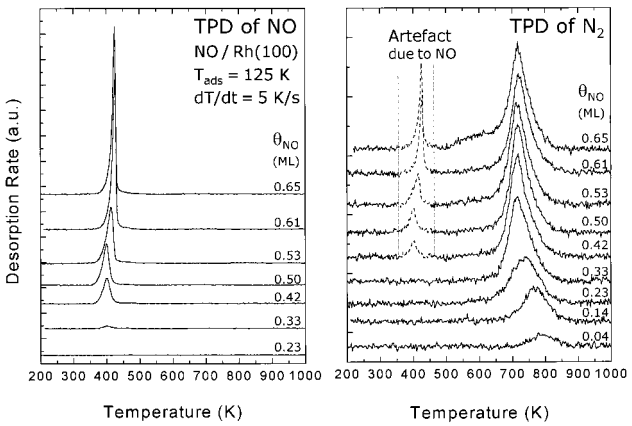


**Figure 1.** TPD spectra of NO ($m/e = 30$) and $N_2$ ($m/e = 28$) after exposing the Rh(100) crystal to various doses of NO at 125 K. The spectra of NO and $N_2$ are not to scale with respect to each other. The heating rate was 5 K/s. The $N_2$ desorption peak at 400−430 K is an artifact, caused by decomposition of NO on the filament of the mass spectrometer.

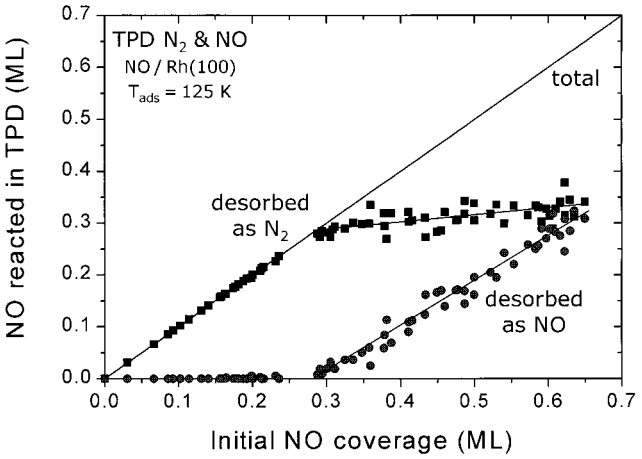


**Figure 2.** Fraction of NO dissociating to form $N_2$ and desorbing intact during temperature programmed reaction of NO on Rh(100) as a function of the initial NO coverage. The data were obtained by quantitation of the TPD spectra in Figure 1.

collected under a polar angle of 50°. To average possible anisotropies in the emission process we applied a target bias of +40 V and an extractor voltage of −300 V on the entrance lens of the quadrupole system. These conditions enable measurements in static mode, with a removal rate of less than one monolayer of adsorbates per hour. The longest experiments lasted 3 min, a typical scan took around 1 min.

The rhodium crystal of (100) orientation with a thickness of about 1.2 mm was mounted on a moveable sample rod by two tantalum wires of 0.3-mm diameter, pressed into small grooves on the side of the crystal. This construction allows for resistive heating to 1450 K. The sample could be cooled to 100 K by flowing liquid nitrogen through the manipulator. Temperatures were measured with a chromel−alumel thermocouple spot-welded to the back of the crystal.

The crystal surface was cleaned by cycles of argon sputtering and annealing under oxygen and UHV. Argon sputtering (1.5 keV, 2 $\mu$A/cm$^2$) at 870 K was used to remove small amounts of impurities, such as boron, sulfur, phosphorus, and chlorine, until these were no longer detectable with auger electron spectroscopy (AES) or SIMS (both positive and negative secondary ions). Carbon appeared to be the most difficult impurity to remove, since it is known to dissolve in the bulk at elevated temperatures (>900 K).[38] Near-surface carbon was removed by heating the crystal in $2 \times 10^{-7}$ mbar $O_2$, cycling the temperature between 900 and 1300 K, until CO and $CO_2$ were absent in TPD spectra taken after saturating the surface with oxygen. Oxygen was removed by annealing the sample to 1425 K.

Nitric oxide (Hoek Loos, 99.5% pure) was used without further purification. Gas dosing for TPD or TPSSIMS measurements was done at 125 K or lower. All temperature programmed experiments were done at a heating rate of 5 K/s.

## III. Results

**1. Temperature Programmed Desorption (TPD).** Temperature programmed desorption spectra, obtained after dosing various amounts of NO on Rh(100) at 125 K, are given in Figure 1. During these experiments, the only desorption products observed were NO ($m/e = 30$), $N_2$ ($m/e = 28$), and $O_2$ ($m/e = 32$); $N_2O$ ($m/e = 44$) was not detected. We show the desorption spectra of NO and $N_2$ only and note that $O_2$ desorbs at higher temperatures (1200−1400 K) with similar peak shapes and desorption temperatures as after adsorption of O-atoms alone.

Before we quantitate these results, we discuss the origin of the peaks in Figure 1. For low NO coverages, $N_2$ and $O_2$ are the only desorbing products, indicating that dissociation of NO is complete at low coverage. At higher coverages, NO desorption is observed as well, and the $N_2$ TPD spectra reveal a second peak at low temperature. A similar peak was observed by several other authors[18,22,24] and labeled as an additional desorption state, $\beta_1$-$N_2$, This state was attributed to a disproportionation reaction between NO and N to form $N_2$ and O-atoms, with $N_2O$ as a possible intermediate.

We believe that this $\beta_1$-$N_2$ state is explained by a reaction of desorbing NO over the filament of the mass spectrometer, for the following reasons:

The low-temperature $N_2$ desorption state appears at exactly the same temperatures and has the same shape as the desorption peak of NO.

Admitting $5 \times 10^{-9}$ mbar of NO in the UHV chamber with the rhodium crystal retracted in the preparation chamber yields mass spectrometric signals of NO ($m/e = 30$), $N_2$ ($m/e = 28$), and $O_2$ ($m/e = 32$) with the former two at the same intensity ratio as for the NO peaks and the low-temperature $N_2$ peaks in Figure 1.

Hence, the low-temperature $N_2$ desorption peaks in the TPD spectra from NO on Rh(100) are fully explained by decomposition of desorbed NO over the filament of the mass spectrometer. After correction for this effect we find no evidence for the disproportionation reaction invoked by previous authors (including from our own group).

*Extent of NO Dissociation.* The initial coverage of NO was determined from the amount of desorbing nitrogen atoms, by integrating the high-temperature $N_2$ (600−800 K) and NO desorption peaks, multiplying the $N_2$ peak area by 2, dividing the NO peak area by the relative difference in mass spectrometer sensitivity for NO and $N_2$ ( = 1.2), and adding these contributions. For the saturation coverage of NO on Rh(100) at 125 K, we use the value of 0.65 monolayer reported by Ho and White.[18]

As summarized in Figure 2, all NO dissociates completely at coverages below 0.28 monolayer, giving rise to desorption of $N_2$ at 650−850 K and $O_2$ at 1200−1400 K. At coverages above 0.28 monolayer NO, the $N_2$ desorption channel appears to be largely saturated: going from an initial NO coverage of 0.28 monolayer to 0.65 monolayer, the amount of N desorbed as $N_2$ in TPD increases only slightly from 0.28 to 0.34 monolayer and almost all NO in excess of 0.28 monolayer

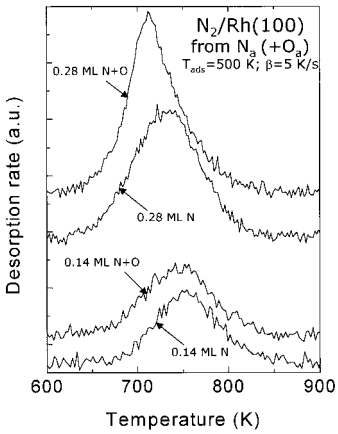


**Figure 3.** $N_2$ desorption spectra measured from dissociated NO ($T_{ads}$ = 500 K) on Rh(100) in the presence and absence of O-atoms. The latter were removed by exposing the surface to CO ($T$ = 500 K, $p_{CO}$ = $2 \times 10^{-8}$ mbar).

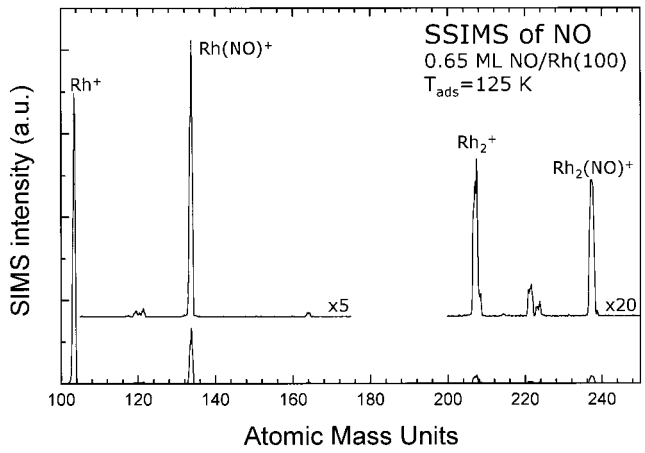


**Figure 4.** SSIMS spectrum of the Rh(100) surface after a saturation dose of NO at 125 K. SSIMS spectra were taken by using a defocused keV $Ar^+$ primary ion beam with a current density of 1 nA/cm$^2$.

desorbs molecularly. At saturation, approximately 52% of the NO dissociates and the remaining 48% desorbs. This is in good agreement with Ho and White,[18] who reported a 54% selectivity to $N_2$. However, different results were found by Siokou et al.,[24] reporting 46% dissociation, and Villarubia and Ho,[22] who found a remarkably higher value of 62% dissociation at saturation coverage. The latter high value may in part have been caused by the fact that Villarubia and Ho included the low $N_2$ desorption peak (see Figure 1) in their quantitation, implying that they significantly overestimated the extent to which NO dissociates. The results of Siokou et al. have most probably been influenced by the presence of atomic carbon on the surface, as visible in a CO contamination peak (which they identified as such) in their $N_2$ TPD spectra.[24] Hence, we conclude that about half (52%) of the NO in an initially saturated adsorbate layer on Rh(100) dissociates upon heating.

*$N_2$ Desorption.* The TPD spectra of $N_2$ in Figure 1 show that $N_2$ is produced in a single peak, which shifts to lower temperatures with increasing coverage. This behavior is typical for second-order desorption kinetics, as expected for recombination of N-atoms to $N_2$. However, the N-atoms recombine on a surface where O-atoms are also present.

To assess the role of coadsorbed oxygen, we prepared oxygen free surfaces covered by atomic N by dissociating NO at 500 K and removing $O_{ads}$ under an ambient CO pressure ($p_{CO} = 2 \times 10^{-8}$ mbar) at 500 K. After this treatment, no surface oxygen could be detected with SSIMS, while $CO_2$ did not form in TPD after CO coadsorption. Figure 3 shows $N_2$ TPD spectra for two different N coverages from stoechiometric amounts of $N_{ads}$ and $O_{ads}$, prepared by dissociative adsorption of NO, and from pure atomic nitrogen, prepared as described above. As Figure 3 shows, the presence of surface oxygen has no noticeable effect on the $N_2$ desorption at a low nitrogen coverage $\theta_N = 0.14$ monolayer. At the higher coverage, 0.28 monolayer of N- and O-atoms each, the oxygen accelerates the $N_2$ desorption.

Analysis of TPD spectra by either the Chan−Aris−Weinberg method[39] or the leading-edge analysis[40] usually yields the most reliable results.[41] Application of the Chan−Aris−Weinberg method for second-order kinetics on the spectra of $N_2$ desorption in the absence of coadsorbed oxygen yields an activation energy of 215 ± 10 kJ/mol and a preexponential factor of $10^{15.1\pm1}$ s$^{-1}$ in the zero coverage limit ($\theta_N = 0$). Leading edge analysis yields values that are slightly higher ($E_{des}$ = 225 ± 5 kJ/mol; $\nu = 10^{15.8\pm0.5}$ s$^{-1}$). These desorption energy values are substantially higher than 180 kJ/mol reported earlier in our laboratory,[24] which may have been caused by the presence of carbon impurities on the surface of the crystal.

*NO Desorption.* For NO coverages between 0.28 and 0.50 monolayer, NO desorbs in a single desorption state around 400 K, which is symmetric by first approximation and which can be described by simple first-order desorption kinetics. For NO coverages higher than 0.50 monolayer, the NO desorption state shifts to higher temperatures up to 430 K at saturation. Also the peak shape shows remarkable changes: at the low-temperature side of the NO desorption state, sharp increase and abrupt decrease at the high-temperature side. Similar phenomena have been observed for NO on Rh(111),[13] but for Rh(100) these features are much more distinct. The activation energy of desorption of NO at an initial coverage of 0.3 monolayer of NO has been determined by Redhead analysis, choosing the same value of the preexponential factor that Borg et al.[13] used for desorption of NO from Rh(111), $\nu = 10^{13.5\pm1}$ s$^{-1}$, yielding $E_{des}$ = 106 ± 10 kJ/mol. Note that this value concerns the desorption of NO in the presence of other species, notably N- and O-atoms.

**2. Static Secondary Ion Mass Spectrometry (SSIMS).** Figure 4 shows a typical static SIMS spectrum of the Rh(100) surface taken after a saturation dose (5 L) of NO at 120 K. The spectrum shows intense substrate peaks of $Rh^+$ at $m/e$ = 103 and $Rh_2^+$ at $m/e$ = 206. Peaks due to adsorbed NO appear at $m/e$ = 30 (not shown) and at the masses of molecular cluster ions such as $Rh(NO)^+$ at $m/e$ = 133 and $Rh_2(NO)^+$ at $m/e$ = 236, while small peaks due to $Rh(NO)_2^+$ at $m/e$ = 163, $Rh_2N^+$ at $m/e$ = 220, and $Rh_2O^+$ at $m/e$ = 222 are observed as well. The high intensity of clusters of the type $Rh_n(NO)^+$ with respect to the intensities of $Rh_nN^+$ and $Rh_nO^+$ indicates that the adsorption of NO on the Rh(100) at 125 K is molecular, in agreement with high-resolution electron-energy-loss spectroscopy (HREELS) studies of NO on Rh(100), which show that dissociation does not occur for temperatures below 170 K.[22] We attribute the small $Rh_2N^+$ and $Rh_2O^+$ peaks to the fragmentation of molecular NO during the secondary ion emission process, in analogy with the presence of $Rh_2N^+$ and $Rh_2O^+$ clusters in SSIMS spectra of molecular NO on Rh(111)[13] and the presence of $Rh_2C^+$ and $Rh_2O^+$ clusters in SSIMS spectra of molecular CO on Rh(111).[42] Finally, the small $Rh(H_2O)^+$ ion cluster ($m/e$ = 121) is due to the adsorption of tiny amounts of water—for which SSIMS is particularly sensitive[42]—originating from the residual gas during cooling and NO adsorption at 125 K.

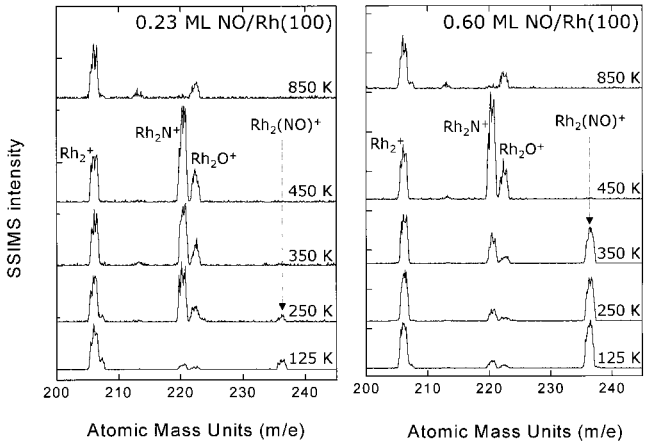


**Figure 5.** SSIMS spectra of a low NO coverage $\theta_{NO} = 0.23$ (left panel) and high coverage $\theta_{NO} = 0.60$ monolayer (right panel), taken after adsorbing NO at 125 K, heating the Rh(100) crystal to the indicated temperature, and subsequent cooling to 200 K. The spectra were normalized to the $Rh_2^+$ intensity to allow for quantitative comparison.

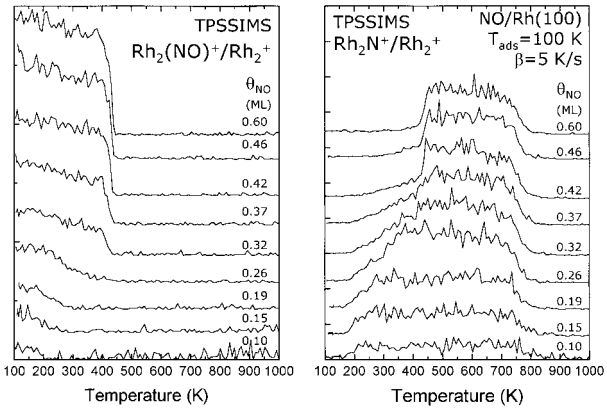


**Figure 6.** TPSSIMS ion intensity ratios $Rh_2(NO)^+/Rh_2^+$ and $Rh_2N^+/Rh_2^+$ during temperature programmed reaction of NO on Rh(100) as a function of initial NO coverage. NO was adsorbed at 125 K and the applied heating rate was 5 K/s.

In general, quantification of SSIMS intensities in terms of adsorbate surface concentrations is best done by considering intensity ratios of suitable secondary ion clusters.[43,44] For example, ratios such as $Rh(NO)^+/Rh^+$ and $Rh_2(NO)^+/Rh_2^+$ often correlate well with the coverage of NO, particularly at low coverages. By taking such ratios, the intensity differences due to different neutralization probabilities at different coverages, caused by differences in work functions,[45,46] usually cancel out satisfactorily.[13,47,48] For the present study, the ratio $Rh_2(NO)^+/Rh_2+$ varied proportionally with coverage for $0 < \theta_{NO} < 0.3$ monolayer and linearly but with a steeper slope for $0.3 < \theta_{NO} < 0.5$ monolayer; at higher coverages, the $Rh_2(NO)^+/Rh_2^+$ becomes more or less constant and does not reflect the actual coverage of NO anymore. Hence, quantitation is possible at coverages up to 0.5 monolayer of NO.

The intensity ratio $Rh_2(NO)^+/Rh_2^+$ is considerably larger than the ratio $Rh(NO)^+/Rh^+$, which, in analogy with work by Vickerman and co-workers on CO,[43] may be taken as evidence that NO binds in sites of high coordination (bridge or 4-fold hollow). This is in agreement with the EELS study of Villarubia and Ho, which excludes linearly bound NO, and with density-functional calculations by Loffreda et al.,[17] which favor the bridge site for NO on Rh(100).

*Decomposition of NO.* To investigate the decomposition of NO, Figure 5 shows static SIMS spectra ($m/e = 200-250$) of NO on Rh(100) after heating to the indicated temperatures. All spectra were normalized to the $Rh_2^+$ intensity for easy comparison. After adsorption at 120 K, the spectra exhibit intense $Rh_2(NO)^+$ peaks, which are characteristic for the presence of molecular NO; the small intensities of $Rh_2N^+$ and $Rh_2O^+$ are attributed to the fragmentation of intact NO during the ion emission process.

Heating the surface with a low coverage of NO [Figure 5 (left panel)] to 250 K results in a decrease of the $Rh_2(NO)^+$ peak and a significant intensity rise of the $Rh_2N^+$ and $Rh_2O^+$ peaks. This, together with the absence of desorption phenomena between 120 and 250 K (see the TPD spectra in Figure 1), indicates that a significant fraction of the NO has dissociated at 250 K. Upon further heating to 350 and 450 K, the $Rh_2(NO)^+$ peak disappears completely, accompanied by a further increase in both the $Rh_2N^+$ and $Rh_2O^+$ peaks. As equal amounts of atomic nitrogen and oxygen are formed upon dissociation and no desorption takes place, it may be concluded that SSIMS is about 4 times more sensitive toward adsorbed $N_{ads}$ than to $O_{ads}$, in agreement with previous SSIMS data of Borg et al.[13] and DeLouise and Winograd.[8] We note that diatomic $RhN^+$ and $RhO^+$ cluster ions were virtually absent in the SSIMS spectra of both isolated and mixed overlayers of atomic N and O, in analogy with SSIMS results of NO on Rh(111).[13] This is related to the fact that nitrogen and oxygen atoms reside in 4-fold hollow sites on the Rh(100) surface,[17,49] which favors the emission of secondary ion clusters containing multiple metal atoms.[43] Heating the crystal to 850 K results in the disappearance of the $Rh_2N^+$ cluster ion, due to desorption of $N_2$, leaving oxygen atoms as the only adsorbate.

The series of SIMS spectra for NO on Rh(100) at a higher coverage of 0.60 monolayer show that dissociation occurs at higher temperatures (Figure 5, right panel). No dissociation has taken place after heating to 250 K, whereas only part of the NO has dissociated at 350 K, as indicated by a small decrease in $Rh_2(NO)^+$ intensity and a concomitant increase of $Rh_2N^+$ and $Rh_2O^+$ intensities. Heating to 450 K is sufficient to remove all molecular NO from the surface, both by dissociation, as evidenced by increase of $Rh_2N^+$ and $Rh_2O^+$ intensities, and by desorption, as evidenced by the TPD spectra in Figure 1. Again, heating to 850 K removes all nitrogen and leaves only oxygen on the surface.

**3. Temperature Programmed Static SSIMS (TPSSIMS).** Monitoring characteristic cluster ion intensities in SSIMS as a function of time by multiplexing the mass spectrometer has proven to be a powerful way to study the kinetics of surface reactions in an at least semiquantitative fashion.[50] Figure 6 shows the intensity ratios $Rh_2(NO)^+/Rh_2^+$ and $Rh_2N^+/Rh_2^+$, characteristic of adsorbed NO and N, respectively, during temperature programmed heating of Rh(100) with different coverages of NO, which was adsorbed at 120 K. The heating rate of 5 K/s was the same as used in TPD, to enable comparisons between TPSSIMS and TPD spectra. For coverages below 0.25 monolayer, the $Rh_2N^+/Rh_2^+$ intensity ratio is linearly proportional to the coverage of atomic nitrogen. Good quantitative agreement exists between the decrease in $Rh_2N^+/Rh_2^+$ intensity ratio between temperatures of 650 and 850 K and the atomic nitrogen coverage as determined from the $N_2$ TPD spectra.

For NO coverages below 0.28 monolayer, where NO desorption does not occur, the decrease of the $Rh_2(NO)^+/Rh_2^+$ ion intensity ratio reflects the dissociation of NO. As Figure 6 shows, dissociation starts at temperatures below 200 K at low NO coverages, as evidenced by the decrease of the $Rh_2(NO)^+/Rh_2^+$ ratio and the concomitant increase in $Rh_2N^+/Rh_2^+$ at

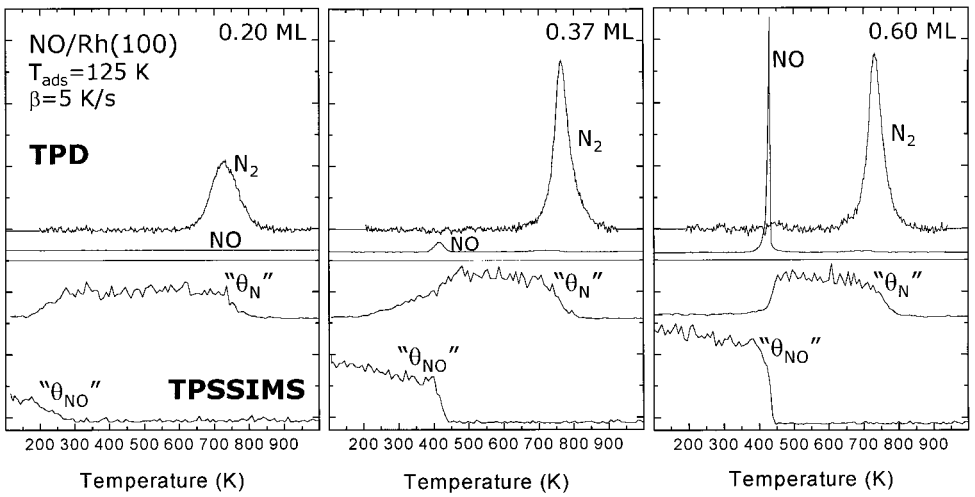


**Figure 7.** Selected NO and $N_2$ desorption rates from Figure 1 (top) and $Rh_2(NO)^+/Rh_2^+$ and $Rh_2N^+/Rh_2^+$ TPSSIMS ion intensity ratios, representing the surface coverages of NO and N-atoms respectively, from Figure 6 (bottom), during temperature programmed reaction of NO on Rh(100), for low (left panel), medium (central panel), and high (right panel) initial NO coverages.

temperatures below 200 K. However, dissociation of NO is progressively retarded at increasing coverages, ultimately to about 425 K for coverages of the order of 0.4 monolayer and higher. The continuous decrease of the $Rh_2N^+/Rh_2^+$ ratio in the temperature range 650−850 K corresponds to the recombination of N-atoms into desorbing $N_2$.

Note that the $Rh_2N^+/Rh_2^+$ signal becomes noisy for temperatures where no molecular NO resides on the surface. The reason is that SIMS intensities are high when the work function of the surface is high. The work function, however, decreases when NO disappears, either by dissociation or desorption. Hence, the absolute SIMS intensities decrease and the statistics deteriorate.

We discuss the dissociation in the intermediate coverage regime, where part of the NO desorbs from the surface, in more detail. For NO coverages exceeding 0.30 monolayer, the decrease in the $Rh_2(NO)^+/Rh_2^+$ intensity ratio reflects dissociation and desorption of NO, hence the dissociation rate is more directly reflected by the $Rh_2N^+/Rh_2^+$ ratio. Clearly, the rate of dissociation is slowed at higher coverages of NO. At low coverage ($\theta_{NO}$ < 0.30 monolayer), there is only one regime from 250 to 400 K where the nitrogen coverage increases continuously with temperature, with the completion of dissociation shifting to higher temperature with increasing coverage. For coverages between 0.30 and 0.50 monolayer, dissociation in this temperature regime is suppressed, and an additional fast dissociation channel appears between 400 and 430 K, as evidenced by the steep increase of the $Rh_2N^+/Rh_2^+$ ratio in this temperature range. This channel coincides with the desorption of NO, which occurs between 400 and 430 K for $\theta_{NO}$ > 0.30 monolayer, as evidenced by the TPD spectra in Figure 1.

At NO coverages close to saturation (0.60 monolayer), dissociation is completely inhibited in the temperature range between 250 and 400 K; dissociation takes place exclusively in the temperature range between 400 and 430 K. In this range, the atomic N coverage increases rapidly and reaches a maximum after 430 K, where it stays constant up to the temperature where $N_2$ desorbs.

## IV. Discussion

**1. Mechanism of NO Decomposition.** The following elementary reactions occur during temperature programmed heating of NO adsorbed on Rh(100):

$$NO_{ads} + * \rightarrow N_{ads} + O_{ads} \qquad T = 170-430 \text{ K, depending on } \theta_{NO} \quad (1)$$

$$NO_{ads} \rightarrow NO + * \qquad T = 400-430 \text{ K, for } \theta_{NO} > 0.28 \text{ monolayer} \quad (2)$$

$$N_{ads} + N_{ads} \rightarrow N_2 + 2* \qquad T = 600-800 \text{ K} \quad (3)$$

$$O_{ads} + O_{ads} \rightarrow O_2 + 2* \qquad T = 1200-1400 \text{ K} \quad (4)$$

This scheme differs from the one proposed by Ho and White,[18] Villarubia et al.,[22] and Siokou et al.[24] in that it does not contain the disproportionation reaction between adsorbed NO and N-atoms to form $N_2$ and $O_{ads}$ around 430 K. The $N_2$ production observed around 430 K in the initial NO coverage regime above 0.28 monolayer can be entirely attributed to decomposition of desorbed NO on the hot filament of the mass spectrometer. Note that the issue has implications for quantitation: inclusion of the low-temperature $N_2$ leads to an overestimate of the NO fraction that dissociates.[22] We believe that this explains why Villarubia and Ho reported a higher fraction of dissociated NO (62%) than the 52% we find in this study.

We will now discuss the kinetics of the individual steps in the scheme above. To facilitate the discussion, Figure 7 compares SIMS and TPD results for three characteristic coverages in the behavior of NO on Rh(100).

*$\theta_{NO}$ < 0.28 Monolayer.* The low coverage range, see Figure 7, is characterized by complete NO dissociation. For the lowest coverages, dissociation starts around 170 K and is completed around 250 K. With increasing coverage, the onset of dissociation shifts slightly to about 200 K. However, the completion of dissociation is significantly retarded to 375 K. Hence, dissociation is retarded due to interactions of the dissociating NO molecule with NO (shift in onset of dissociation from 170 to 200 K), and with the atomic adsorbates, $N_{ads}$ and $O_{ads}$, which retard the dissociation up to 375 K. Hence the adsorbed atoms appear to affect the dissociation of NO most.

*0.28 < $\theta_{NO}$ < ~0.50 Monolayer.* In the medium coverage range, NO dissociates until all sites are occupied, after which the remaining NO starts to desorb when the temperature reaches

about 400 K. Additional NO dissociates on the empty sites freed by desorption of NO, due to the creation of vacancies in the relatively small temperature regime between 400 and 430 K. The effect is best seen in the increase in the SIMS intensity ratio characteristic of atomic nitrogen, $Rh_2N^+/Rh_2^+$, since the decrease in the corresponding signal for NO reflects both desorption and dissociation. Note that the desorbing NO molecules do so from an environment containing atomic and molecular species.

*~0.50 Monolayer < $\theta_{NO}$ ≤ 0.65 Monolayer.* At coverages close to saturation, dissociation is self-inhibited until desorption of NO takes place at temperatures above 400 K. Here desorption and dissociation of NO occur rapidly in a narrow temperature region. The onset of NO desorption is delayed by ca. 25 K (from ~375 K at 0.40 monolayer to ~400 K at 0.60 monolayer), which we attribute to the absence of atomic species and the associated repulsive N−NO and O−NO interactions. Note that at the onset of the desorption, at 400 K, NO molecules leave from an environment of NO molecules. As discussed above, desorption of NO from a mixed environment of atomic and molecular species starts at 375 K already. Apparently, repulsion between NO molecules is smaller than repulsion between NO and its dissociation products. The remarkably sharp shape of the NO desorption peak and the steep increase in the SIMS signal for atomic nitrogen in Figure 7 can now be explained by an autocatalytic mechanism and the delicate interplay of repulsive interactions: as soon as the first NO molecules desorb, empty sites become available for dissociation. Since dissociation of NO is a very rapid process at this temperature, these empty sites are filled instantaneously by $N_{ads}$ and $O_{ads}$. These atoms enhance the NO desorption rate, and more empty sites become available. This mechanism results in an explosive increase in the rates for both desorption and dissociation until all NO has disappeared from the surface.

Hence the rate of NO dissociation on Rh(100) is strongly affected by several factors, such as the availability of vacant sites and lateral interactions between the dissociating molecule and coadsorbed NO, N, and O. We will therefore determine the kinetic parameters for the dissociation step in the limit of zero coverage and describe the effects of coverage in a qualitative fashion. As adsorbate coverages from the SIMS intensity ratios can only reliably be obtained at low coverages, we restrict the determination of the kinetic parameters to the regime of $\theta_{NO}$ < 0.28 monolayer.

**2. Kinetic Parameters of NO Dissociation.** Figure 8 shows the coverages of $NO_{ads}$ and $N_{ads}$ as derived from the corresponding TPSSIMS ion intensity ratios as a function of temperature during a 5 K/s heating ramp, starting from molecular NO adsorbed at 125 K. We discuss different approaches to model the curves in Figure 8. The first try is based on the requirement of an ensemble of *n* empty sites for dissociation and kinetic parameters that are independent of coverage, similarly as reported by Borg et al.[13] for NO on Rh(111), as expressed in the following differential equation:

$$r_{dis} = -\frac{d(\theta_{NO}/\theta_{sat})}{dT} = \frac{\nu_{dis}}{\beta}\frac{\theta_{NO}}{\theta_{sat}}\left(\frac{\theta_*}{\theta_{sat}}\right)^n \exp\left(-\frac{E_{dis}}{RT}\right) \quad (5)$$

where $\theta_{NO}$ and $\theta_*$ are the absolute coverages (in monolayer) of NO and vacant sites, respectively, $\theta_{sat}$ is the total saturation coverage of O- and N-atoms, 0.66 monolayer, equivalent to the maximum amount of NO that can dissociate, $\nu_{dis}$ ($s^{-1}$) and $E_{dis}$ (kJ/mol) are the preexponential factor and activation energy for dissociation, respectively, and $\beta$ is the heating rate. The parameter *n* represents the number of sites in the ensemble required for dissociation of NO. This differential equation was integrated numerically for independent values of the preexponential factor and activation energy to obtain the best fit for both the measured $NO_{ads}$ and $N_{ads}$ coverages.

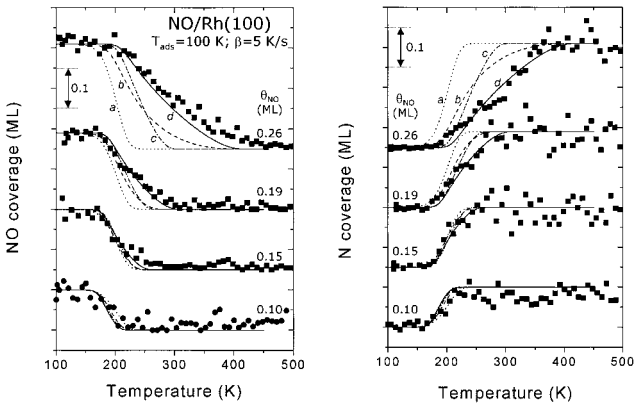


**Figure 8.** Dissociation kinetics of 0.10, 0.15, 0.19, and 0.26 monolayer (initial coverage increasing from top to bottom) NO on Rh(100), as monitored with TPSSIMS by the decrease of the NO coverage (l; left panel) and the complementary increase of the N coverage (n; right panel). The different coverages have been offset. The lines are fits assuming (a) pure first-order kinetics ($E_{dis}$ = 18 ± 6 kJ/mol, $\nu_{dis}$ = $10^{4\pm1}$ $s^{-1}$, $\theta_{sat}$ = 0.66 monolayer), (b) an NO molecule requiring an ensemble of six vacant sites (*n* = 6) for dissociation ($E_{dis}$ = 25 ± 6 kJ/mol, $\nu_{dis}$ = $10^{7\pm1}$ $s^{-1}$, $\theta_{sat}$ = 0.66 monolayer), (c) an ensemble of only one vacant site (*n* = 1), $\nu_{dis}$ = $10^{11\pm1}$ $s^{-1}$, and a linear increase of $E_{dis}$ with total coverage [$E_{dis}(\theta_{tot}) = E_{dis,0} + \alpha\theta_{tot}$ kJ/mol with $E_{dis,0}$ = 23 ± 6 kJ/mol, α = 100, $\theta_{sat}$ = 1 monolayer], (d) an ensemble of one vacant site (*n* = 1), $\nu_{dis}$ = $10^{11\pm1}$ $s^{-1}$, and a quadratic increase of $E_{dis}$ with total coverage [$E_{dis}(\theta_{tot}) = E_{dis,0} + \alpha\theta_{tot}^2$ kJ/mol with $E_{dis,0}$ = 23 ± 6 kJ/mol, α = 175, $\theta_{sat}$ = 1 monolayer].

The fits indicated by dotted lines correspond to the case of *n* = 0 and ignore any ensemble requirement. Clearly, these fits are unacceptable for higher coverages. Including the site requirement in the kinetics by increasing the value of *n* improves the fits somewhat (the fit corresponding to *n* = 6 is shown as the dashed line in Figure 7) and leads to kinetic parameters $E_{dis}$ = 20 ± 5 kJ/mol and $\nu_{dis}$ = $10^{5\pm1.5}$ $s^{-1}$ for *n* = 2, $E_{dis}$ = 23 ± 5 kJ/mol and $\nu_{dis}$ = $10^{6\pm1.5}$ $s^{-1}$ for *n* = 4, and $E_{dis}$ = 25 ± kJ/mol and $\nu_{dis}$ = $10^{7\pm1.5}$ $s^{-1}$ for *n* = 6.

All these fits based on site blocking are not acceptable, however, because the preexponential factors well below $10^{10}$ $s^{-1}$ are inconsistent with transition state theory.[51−53] Also, ensemble sizes of up to six free sites are hard to reconcile with the result that 52% of the NO dissociates. Experimental preexponential factors for dissociation of different diatomic molecules on various metal surfaces have been found to fall between $10^9$ and $10^{12}$ $s^{-1}$.[54] Calculations on the dissociation of CO and NO on Cu(100) and Cu(111) cluster models by van Daelen et al.[55,56] predict that the entropy loss when going from a perpendicularly adsorbed NO molecule to a constrained, inclined transition state results in preexponential factors of $10^{11}$−$10^{12}$ $s^{-1}$. Hence, site blocking can only partially account for the inhibition of NO dissociation on Rh(100) at increasing coverages.

As coadsorbed NO and coadsorbed N- and O-atoms clearly affect the dissociation in different ways, it is obvious that the effective activation barrier $E_{dis}$ for NO dissociation is affected by interactions with coadsorbed species. This is confirmed by bond-order conservation Morse potential (BOCMP) calculations by Shustorovich and Bell,[36] who found an increase in the activation energy for dissociation of NO on Rh(100) from 34

kJ/mol on an empty surface to 107 kJ/mol for a surface covered with a c(2 × 2)-array of N- and O-atoms, respectively.

A rigorous description of the effect of lateral interactions on the kinetics requires the incorporation of local geometries in a Monte Carlo simulation.[16,35] Such studies are in progress. Here we describe the effect of lateral interactions in an empirical way by assuming the following relation between the activation barrier for dissociation and the total adsorbate coverage:

$$E_{dis}(\theta_{tot}) = E_{dis,o} + \alpha\theta_{tot}^{m} \quad (6)$$

where $E_{dis}(\theta_{tot})$ is the activation barrier for dissociation of NO as a function of total coverage, $E_{dis,0}$ is the activation barrier at zero coverage, $\alpha$ is a constant, $\theta_{tot}$ is the total adsorbate coverage $\theta_{NO} + \theta_N + \theta_O$, and $m$ is an integer. Increasing $m$ above unity provides an artificial means to stress that the effect of lateral interactions becomes particularly apparent at higher total coverages. The differential eq 5 was numerically solved for independent values of $E_{dis,0}$ and $\alpha$ to obtain the best fit over the measured temperature range for the different coverages. The preexponential factor $\nu_{dis}$ was kept fixed at $10^{11}$ $s^{-1}$, in agreement with theory.[55,56] Site blocking was modeled by assuming that dissociation of an NO molecule requires one vacancy ($n = 1$); larger ensemble sizes ($n > 1$) heavily restrict the total amount of NO that can be dissociated. The total number of sites available, $\theta_{sat}$ in (5), was fixed at a complete monolayer, implying that in principle all 4-fold hollow sites can be occupied by NO, N, and O. This seems the most realistic approach, because all 4-fold sites have the same geometry, hence the same reactivity.

Figure 8 shows a number of fits based on (6). First, ignoring all lateral interactions by keeping the activation energy the same for all coverages (dotted line in Figure 8) grossly overestimates the rate of dissociation at low temperatures. Choosing a linear relation between activation energy and coverage yields the dash−dotted line; also this results in too much dissociation at too low temperatures. Increasing the value of $m$ in (6) to 2 stresses that lateral interactions become notably present at higher coverages, when near-neighbor sites of the dissociating NO molecule become progressively more occupied. The solid line in Figure 8 corresponds to $E_{dis,0} = 37$ kJ/mol, $m = 2$, and $\alpha = 175$. Without associating any other physical meaning to $\alpha$ and $m$, we conclude that the notion of lateral interactions coming into play at higher coverages leads to an acceptable description of the coverage dependence of the NO dissociation rate. This description accounts for continuously increasing lateral repulsion in the adlayer with increasing coverage. This appears to be reasonable since at low coverages NO can diffuse easily over the surface to find an empty site for dissociation without neighboring atoms or molecules. Hence dissociation will not be seriously affected at low coverage but becomes increasingly hindered at higher coverages. We note that the activation energy for NO dissociation on Rh(100) in the limit of zero coverage, 37 ± 3 kJ/mol, is in good agreement with the 34 kJ/mol predicted by Shustorovich and Bell.[36] The value of 44 ± 3 kJ/mol reported by Villarubia and Ho,[22] valid at a NO coverage of 0.15 monolayer, agrees very well with the value derived from (6) for the same coverage.

**3. Kinetics of $N_2$ and NO Desorption.** The $N_2$ TPD spectra obtained upon heating an NO adlayer on Rh(100) show only one $N_2$ desorption state, originating from recombination of surface N atoms between 600 and 800 K. The rate of desorption is accelerated by the presence of atomic O, when the total coverage is high, as evidenced by the experiment at $\theta_N = \theta_O = 0.28$ monolayer in Figure 3. At this coverage, the presence of $O_{ads}$ has a distinct repulsive effect on the desorption of $N_2$, however. Due to atomic oxygen, the $N_2$ desorption peak is sharpened and the peak maximum is shifted to lower temperature. More important, the high-temperature side (trailing edge) of the $N_2$ desorption trace has shifted to lower temperatures, which is a strong indication for increased repulsion in the mixed $N_{ads} + O_{ads}$ adlayer. This can be easily rationalized, since atomic N and atomic O both compete for the 4-fold hollow sites.[17,49] In addition, we cannot exclude the possibility that a surface reconstruction influences the $N_2$ desorption kinetics at higher coverages as well. The square lattice of the Rh(100) surface is reported to undergo a clockwise−anticlockwise reconstruction upon adsorption of 0.50 monolayer of atomic O.[57,58] We conclude on the basis of the oxygen coadsorption experiments that the desorption parameters for second order $N_2$ desorption, 215 ± 10 kJ/mol and $10^{15.1\pm1}$ $s^{-1}$, obtained at coverages of $\theta_N = \theta_O = 0.15$ monolayer and lower are not affected by lateral interactions between N and O atoms.

Finally, the desorption of NO is necessarily affected by the presence of coadsorbed species. Repulsion by N and O atoms has a stronger effect than repulsion by coadsorbed NO. The desorption parameters $\nu = 10^{13.5\pm1}$ $s^{-1}$ and $E_{des} = 106 \pm 10$ kJ/mol describe desorption of NO in the presence of $N_{ads}$ and $O_{ads}$, implying that the actual heat of adsorption of NO on an empty Rh(100) will be considerably higher than this value. Indeed, Loffreda et al.[17] calculate adsorption energies on the order of 200 kJ/mol for NO in (2 × 2) structure on Rh(100) (−2.18 eV for adsorption on bridge sites, −1.82 eV for NO in the 4-fold hollow site). Thus lateral interactions play a decisive role in the selectivity of the NO decomposition. At low coverage, the activation barrier for dissociation ($E_{dis}$) is much lower than the barrier for desorption ($E_{des}$), resulting in complete dissociation and subsequent complete conversion to $N_2$. With increasing coverage and thus increasing lateral repulsion in the adlayer, $E_{dis}$ increases, slowing down the rate of dissociation. On the other hand, $E_{des}$ decreases, in particular by repulsion between NO and its decomposition products. When ca. 0.28 monolayer of NO is decomposed, dissociation and desorption of NO become competing processes with $E_{dis} \approx E_{des}$. Since the preexponential factor for desorption is 2−3 orders larger than that for dissociation, desorption will prevail.

**4. Comparison of NO Dissociation and $N_2$ Desorption on Rh(100) and Rh(111).** The decomposition and desorption of NO on Rh(100) shows many similarities with the same reactions on the more densely packed Rh(111) surface. On both surfaces, NO adsorbs molecularly at low temperatures, and upon heating the NO at small coverages ($\theta_{NO} < 0.25$ monolayer), dissociation to $N_{ads}$ and $O_{ads}$ is complete. On both surfaces, nitrogen atoms exclusively recombine to form $N_2$ and formation of $N_2O$ is not observed under UHV conditions. The activation energies for dissociation of NO and desorption of $N_2$, however, differ substantially, see Table 1.

Dissociation proceeds much faster on Rh(100) than on Rh(111), as is best seen by comparing the TPSSIMS spectra reported here with those obtained by Borg et al.,[13] especially in the low coverage limit ($\theta_{NO} < 0.15$ monolayer) where lateral interactions play a minor role. Whereas on Rh(100) dissociation of NO starts around 170 K and is completed around 250 K, dissociation on Rh(111) only starts around 250 K and is finished around 350 K. This clearly shows that the more open Rh(100) surface is intrinsically more active in the dissociation of NO than the densely packed Rh(111) surface.

At higher NO coverages, dissociation of NO is no longer complete and part of the NO desorbs intact. On both surfaces,

**TABLE 1: Kinetic Parameters for the Elementary Reaction Steps Involved in the Thermal Decomposition and Desorption of NO on Rh(100) and Rh(111)**

| | Rh(111) | | Rh(111) | | |
|---|---|---|---|---|---|
| elementary reaction | $E_{act}$, kJ/mol | $\nu$, $s^{-1}$ | $E_{act}$, kJ/mol | $\nu$, $s^{-1}$ | remarks |
| $NO_{ads} + * \rightarrow N_{ads} + O_{ads}$ | $65 \pm 6$ | $10^{11\pm1.0}$ | $37 \pm 3$ | $10^{11\pm1.0}$ | low coverage limit |
| $NO_{ads} \rightarrow NO_{gas} + *$ | $113 \pm 10$ | $10^{13.5\pm1.0}$ | $106 \pm 10$ | $10^{13.5\pm1.0}$ | at $\theta_N = \theta_O = 0.25$ monolayer for Rh(111) 0.28 monolayer for Rh(100) |
| $N_{ads} + N_{ads} \rightarrow N_2 + 2*$ | $118 \pm 10$ | $10^{10\pm1.0}$ | $225 \pm 5$ | $10^{15.8\pm0.5}$ | low coverage limit |

dissociation and desorption of NO are highly coverage dependent, due to the requirement of an ensemble of one or more vacant sites and also because dissociation is inhibited by the decomposition products $N_{ads}$ and $O_{ads}$. The latter is particularly apparent in the present study, as discussed in relation with Figure 8. At saturation coverage, dissociation is completely blocked on both surfaces and is delayed until NO desorption (~400 K) produces free sites.

The activation barrier and also the preexponential factor for nitrogen formation on Rh(100) are much higher than on Rh(111); see Table 1. We have no explanation for the large difference in the preexponential factor. We cannot exclude the role of an inhomogeneous distribution of the N-atoms[15] and the involvement of surface reconstruction.[57,58] The higher activation energy for $N_2$ desorption on Rh(100), however, is in agreement with the stronger bonding of atomic adsorbates on more open surfaces[51] as, e.g., observed in calorimetric measurements for adsorption of oxygen on different surfaces of nickel.[59−62]

Under the assumption that preexponential factors are equal ($\nu = 10^{13.5}$ $s^{-1}$), there is only a small difference in the activation barrier for NO desorption from the two crystal surfaces. Desorption of NO on Rh(100) occurs only a 15−25 K earlier than on Rh(111). This effect is relatively small when compared with the temperature shifts observed for dissociation and $N_2$ formation on the different crystal faces. As explained elsewhere, the nature of the bonding of molecules such as CO and NO, with counteracting contributions from the $5\sigma$ and the $2\pi^*$ orbitals, forms the reason that adsorption energies of these molecules vary generally much less with crystal structures than those of atoms.[51]

Figure 9 summarizes the energetics of the reactions in a schematical energy diagram. The heats of adsorption of NO, N, and O have been taken from the density-functional slab calculations using periodic boundary conditions by Loffreda et al.[17] and the activation energies from Borg et al.[13] and this work. The calculated adsorption energies are believed to be accurate within 20 kJ/mol for NO and within 10 kJ/mol for the atoms.

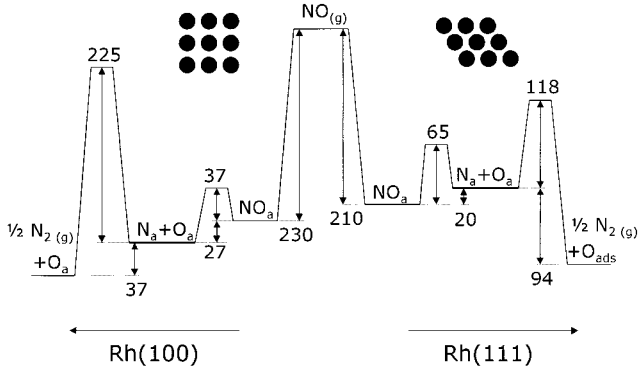


**Figure 9.** Energy diagram comparing the decomposition of NO and the formation of $N_2$ on Rh(100) and Rh(111). Adsorption energies ($\theta_{NO}$ = 0.25 monolayer) are taken from the work of Loffreda et al.[17] and activation energies for dissociation of NO and formation of $N_2$ on Rh(111) from Borg et al.[13] Activation energies on Rh(100) were taken from this work.

The higher heats of adsorption of N- and O-atoms on the Rh(100) surface form the key factor why the energy barrier for dissociation of NO is lower on this surface.

In conclusion, we note that the combination of TPSSIMS, which successfully monitors the decomposition of NO, with TPD, to follow the desorption of NO and $N_2$, has provided a rather complete picture of the reactions of NO on the surface of rhodium at various adsorbate coverages. The results of this work will be used in a subsequent study where Monte Carlo simulations will be used to incorporate the effect of lateral interactions on the kinetics of NO dissociation and reactions of NO with CO. These simulations indicate that pairwise repulsive energies between either of the atoms, N and O, and molecular NO are on the order of 10−15 kJ/mol. The simulations also underline the importance of NO diffusion enabling the NO molecule to move to sites where the repulsion by N- and O-atoms is minimal.

## V. Conclusions

Temperature programmed heating of NO adsorbed on Rh(100) as investigated by desorption and static secondary ion mass spectrometry reveals the following:

NO present at low coverages dissociates between 170 and 250 K, corresponding to an activation energy of 37 kJ/mol at a prefactor of $10^{11}$ $s^{-1}$.

At higher coverages the onset of dissociation shifts to slightly higher temperatures, indicating that neighboring NO molecules have a relatively weak effect on the dissociation process. The temperatures at which dissociation is complete, however, increases considerably, providing evidence that N- and O-atoms retard the dissociation significantly. The activation energy of dissociation increases appreciable faster than expected on the basis of a linear relation with coverage as is often used in mean-field kinetic descriptions.

The existence of a disproportionation reaction between adsorbed NO and N to $N_2$ and O, as invoked by several authors, can entirely be excluded under UHV conditions.

NO dissociates faster on Rh(100) (37 kJ/mol) than on Rh(111) (65 kJ/mol), but formation of $N_2$ is much slower on Rh(100) (215 kJ/mol) than on Rh(111) (120 kJ/mol).

**Acknowledgment.** This work was financially supported by The Netherlands Organization for Scientific Research—Chemical Sciences (NWO−CW) and performed under the auspices of The Netherlands Institute of Catalysis Research (NIOK).

## References and Notes

(1) Taylor, K. C. *Catal. Rev.−Sci. Eng.* **1993**, *35*, 457.
(2) Papapolymerou, G. A.; Schmidt, L. D. *Langmuir* **1985**, *1*, 488.
(3) Hendrickx, H. A. C. M.; Nieuwenhuys, B. E. *Surf. Sci.* **1986**, *175*, 185.
(4) Sellmer, C.; Schmatloch, V.; Kruse, N. *Catal. Lett.* **1995**, *35*, 165.
(5) Campbell, C. T.; White, J. M. *Appl. Surf. Sci.* **1978**, *1*, 347.
(6) Castner, D. G.; Sexton, B. A.; Somorjai, G. A. *Surf. Sci.* **1978**, *71*, 519.
(7) Root, T. W.; Schmidt, L. D.; Fisher, G. B. *Surf. Sci.* **1983**, *134*, 30.

(8) DeLouise, L. A.; Winograd, N. *Surf. Sci.* **1985**, *159*, 199.
(9) Root, T. W.; Fisher, G. B.; Schmidt, L. D. *J. Chem. Phys.* **1986**, *85*, 4679.
(10) Root, T. W.; Fisher, G. B.; Schmidt, L. D. *J. Chem. Phys.* **1986**, *85*, 4687.
(11) Bugyi, L.; Solymosi, L. *Surf. Sci.* **1987**, *188*, 475.
(12) Kao, C.-T.; Blackman, G. S.; van Hove, M. A.; Somorjai, G. A.; Chan, C.-M. *Surf. Sci.* **1989**, *224*, 77.
(13) Borg, H. J.; Reijerse, J. P. C.-J. M.; van Santen, R. A.; Niemantsverdriet, J. W. *J. Chem. Phys.* **1994**, *101*, 10052.
(14) Kim, Y. J.; Thevuthasan, S.; Herman, G. S.; Peden, C. H. F.; Chambers, S. A.; Belton, D. N.; Permana, H. *Surf. Sci.* **1996**, *359*, 269.
(15) Xu, H.; Ng, K. Y. S. *Surf. Sci.* **1996**, *365*, 779.
(16) van Hardeveld, R. M.; Hopstaken, M. J. P.; Lukkien, J. J.; Hilbers, P. A. J.; Jansen, A. P. J.; van Santen, R. A.; Niemantsverdriet, J. W. *Chem. Phys. Lett.* **1999**, *302*, 98.
(17) Loffreda, D.; Simon, D.; Sautet, P. *J. Chem. Phys.* **1998**, *108*, 6447.
(18) Ho, P.; White, J. M. *Surf. Sci.* **1984**, *137*, 103.
(19) Ho, P.; White, J. M. *Surf. Sci.* **1984**, *137*, 117.
(20) Villarubia, J. S.; Richter, L. J.; Gurney, B. A.; Ho, W. *J. Vac. Sci. Technol., A* **1986**, *4*, 1487.
(21) Hendershot, R. E.; Hansen, R. S. *J. Catal.* **1986**, *98*, 150.
(22) Villarubia, J. S.; Ho, W. J. *Chem. Phys.* **1987**, *87*, 750.
(23) van Tol, M. F. H.; Nieuwenhuys, B. E. *Appl. Surf. Sci.* **1993**, *67*, 188.
(24) Siokou, A.; van Hardeveld, R. M.; Niemantsverdriet, J. W. *Surf. Sci.* **1998**, *402*−*404*, 110.
(25) Baird, R. J.; Ku, R. C.; Wynblatt, P. *Surf. Sci.* **1980**, *97*, 346.
(26) Bowker, M.; Guo, Q.; Joyner, R. W. *Surf. Sci.* **1991**, *257*, 33.
(27) Cautero, G.; Astaldi, C.; Rudolf, P.; Kiskinova, M.; Rosei, R. *Surf. Sci.* **1991**, *258*, 44.
(28) Schmatloch, V.; Kruse, N. *Surf. Sci.* **1992**, *269/270*, 488.
(29) Schmatloch, V.; Jirka, I.; Kruse, N. *Surf. Sci.* **1993**, *297*, L100.
(30) Comelli, G.; Dhanak, V. R.; Pangher, N.; Paolucci, G.; Kiskinova, M.; Rosei, R. *Surf. Sci.* **1994**, *317*, 117.
(31) Lizzit, S.; Baraldi, A.; Cocco, D.; Comelli, G.; Paolucci, G.; Rosei, R.; Kiskinova, M. *Surf. Sci.* **1998**, *410*, 228.
(32) van Santen, R. A.; Neurock, M. *Catal. Rev.*−*Sci. Eng.* **1995**, *37*, 557.
(33) de Koster, A.; van Santen, R. A. *Surf. Sci.* **1990**, *233*, 366.
(34) de Koster, A.; van Santen, R. A. *J. Vac. Sci. Technol., A* **1988**, *6*, 1128.
(35) van Hardeveld, R. M.; Lukkien, J. J.; Hilbers, P. A. J.; Jansen, A. P. J.; van Santen, R. A.; Niemantsverdriet, J. W., to be published.
(36) Shustorovich, E.; Bell, A. T. *Surf. Sci.* **1993**, *289*, 127.
(37) Belton, D. N.; DiMaggio, C. L.; Schmieg, S. J.; Ng, K. Y. S. *J. Catal.* **1995**, *157*, 559.
(38) Castner, D. G.; Somorjai, G. A. *Surf. Sci.* **1979**, *83*, 60.
(39) Chan, C.-M.; Aris, R.; Weinberg, W. H. *Appl. Surf. Sci.* **1978**, *1*, 360.
(40) Habenschaden, E.; Küppers, J. *Surf. Sci.* **1984**, *138*, L147.
(41) de Jong, A. M.; Niemantsverdriet, J. W. *Surf. Sci.* **1990**, *223*, 355.
(42) Delouise, L. A.; Winograd, N. *Surf. Sci.* **1984**, *138*, 417.
(43) Brown, A.; Vickerman, J. C. *Surf. Sci.* **1982**, *117*, 154; **1983**, *124*, 267; **1985**, *151*, 319.
(44) Borg, H. J.; Niemantsverdriet, J. W. *Catalysis, Specialist Periodical Report*; Eds. Spivey, J. J., Agarwal, A. K., Eds.; The Royal Society of Chemistry: Cambridge, 1994; Vol. 11, p 1.
(45) Nørskov, J. N.; Lundqvist, B. I. *Phys. Rev. B* **1979**, *19*, 5661.
(46) Niemantsverdriet, J. W. *Spectroscopy in Catalysis*, 1st ed.; VCH: Weinheim, 1993; Chapter 4.
(47) Borg, H. J.; van Hardeveld, R. M.; Niemantsverdriet, J. W. *J. Chem. Soc., Faraday Trans.* **1995**, *91*, 3679.
(48) van Hardeveld, R. M.; van Santen, R. A.; Niemantsverdriet, J. W. *J. Phys. Chem. B* **1997**, *101*, 998.
(49) Dubois, L. H. *J. Chem. Phys.* **1982**, *77*, 5228.
(50) van Hardeveld, R. M.; Borg, H. J.; Niemantsverdriet, J. W. *J. Mol. Catal. A: Chem.* **1998**, *131*, 199.
(51) van Santen, R. A.; Niemantsverdriet, J. W. *Chemical Kinetics and Catalysis*, 1st ed.; Plenum Press: New York, 1995; Chapters 3 and 4.
(52) Zhdanov, V. P.; Pavlícek, J.; Knor, Z. *Catal. Rev.-Sci. Eng.* **1988**, *30*, 501.
(53) Zhdanov, V. P. *Surf. Sci. Rep.* **1991**, *12*, 183.
(54) Campbell, C. T.; Sun, Y.-K.; Weinberg, W. H. *Chem. Phys. Lett.* **1991**, *179*, 53.
(55) van Daelen, M. A.; Li, Y. S.; Newsam, J. M.; van Santen, R. A. *Chem. Phys. Lett.* **1994**, *226*, 100.
(56) van Daelen, M. A.; Li, Y. S.; Newsam, J. M.; van Santen, R. A. *J. Phys. Chem.* **1996**, *100*, 2279.
(57) Oed, W.; Dötsch, B.; Hammer, L.; Heinz, K.; Müller, K. *Surf. Sci.* **1988**, *207*, 55.
(58) Mercer, J. R.; Finetti, P.; Leibsle, F. M.; McGrath, R.; Dhanak, V. R.; Baraldi, A.; Prince, K. C.; Rosei, R. *Surf. Sci.* **1996**, *352*−*354*, 173.
(59) Stuckless, J. T.; Wartnaby, C. E.; Al-Sarraf, N.; Dixon-Warren, St. J. B.; Kovar, M.; King, D. A. *J. Chem. Phys.* **1997**, *106*, 2012.
(60) Al-Sarraf, N.; King, D. A. *Surf. Sci.* **1994**, *307*−*309*, 1.
(61) Al-Sarraf, N.; Stuckless, J. T.; Wartnaby, C. E.; King, D. A. *Surf. Sci.* **1993**, *283*, 427.
(62) Vattuone, L.; Yeo, Y. Y.; King, D. A. *J. Chem. Phys.* **1996**, *104*, 8096.